Improving quarkonia invariant mass resolution by measuring the response function of the ALICE muon spectrometer's trajectography chambers

Stanislas Lambert

Under the supervision of : M. Guilbaud & P. Pillot

Faculté de physique et ingénierie
Université de Strasbourg

master Physique Subatomique Astroparticules

Subatech

ALICE

Summary

- **Context**
- **Procedure**
- **Preliminary results**
- **Resolutions**
- **Conclusion & Outlook**

Context - Quark-Gluon Plasma (QGP)

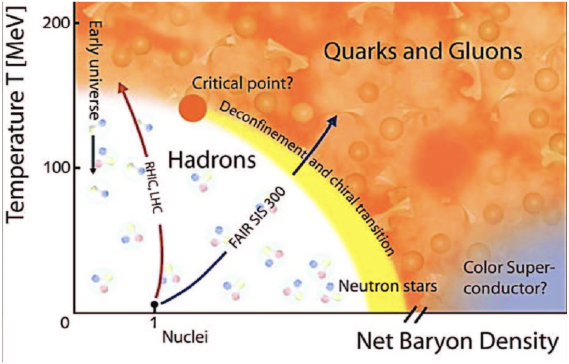

Illustration of the phase diagram of QCD matter

→ quarks and gluons deconfinement ($\alpha_S << 1$)
→ net baryon density $\simeq 0$ (at LHC)
→ $k_B T_c \simeq 155$ MeV (LQCD)
→ $\simeq 10$ fm/c (3.10^{-23}s) (at LHC)

Context - Quarkonia in QGP

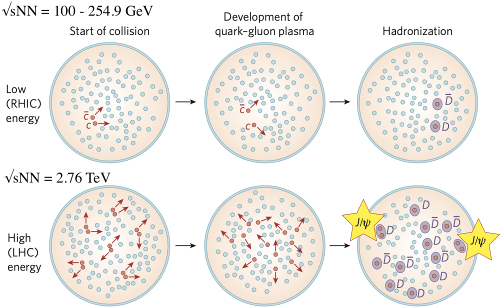

suppression & recombination of charmonia in a QGP

- heavy quark weakly bound states ($c\overline{c}$ and $b\overline{b}$)
- produced at the early stages of the collision
- charmonia/bottomonia as a (hard) probe

$$J/\psi(1S) \rightarrow \mu^+\mu^- \ (5.961 \pm 0.033)\%$$
$$\Upsilon(1S) \rightarrow \mu^+\mu^- \ (2.48 \pm 0.05)\%$$

Context - Motivation

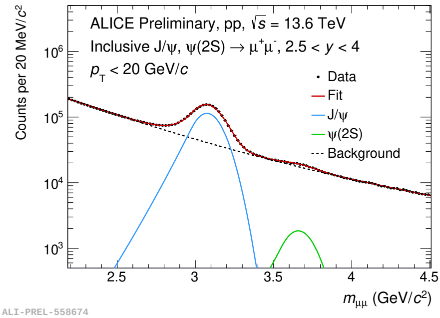

invariant mass of J/ψ and $\psi(2S)$, ALICE Run 3

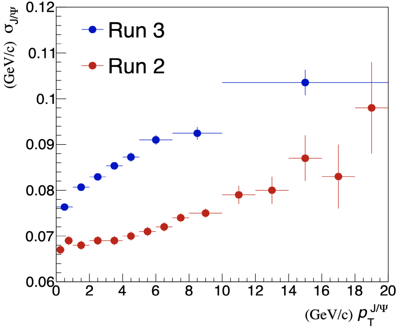

invariant mass resolution of J/ψ for different $p_T^{J/\psi}$ obtained by ALICE

Context - A Large Ion Collider Experiment (ALICE)

→ One of the four major experiments at the CERN's LHC
→ Dedicated to the QGP

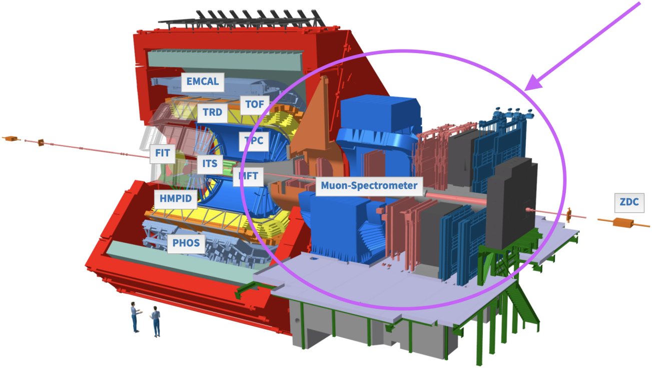

ALICE detector overview

Context - Muon Spectrometer

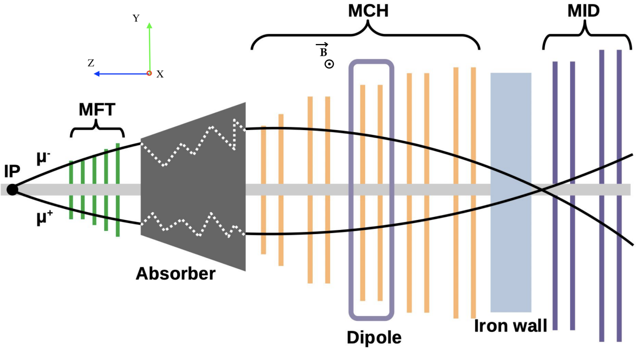

Overview of the Muon Spectrometer with the Muon Forward Tracker (MFT)

- $-4 < \eta < -2.5$
- **M**uon **ID**entifier : detect μ crossing the iron wall
- **M**uon **CH**ambers : 5 stations $\rightarrow$ 10 chambers

Context - Muon Chambers

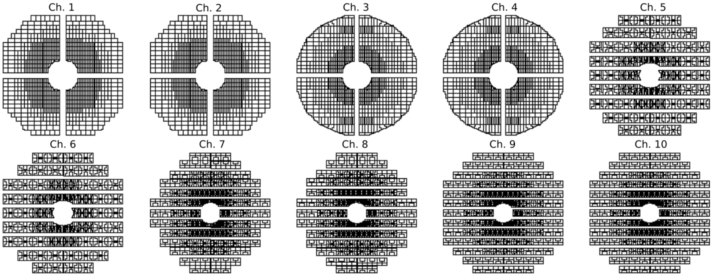

Geometry of the Muon Chambers (MCH)

→ Each chamber is divided into parts :

- Quadrants (Ch. 1-4)
- Slats (Ch. 5-10)

→ Each segmentation (within a part) has a pad arrangement

Context - Inside the Muon Chambers

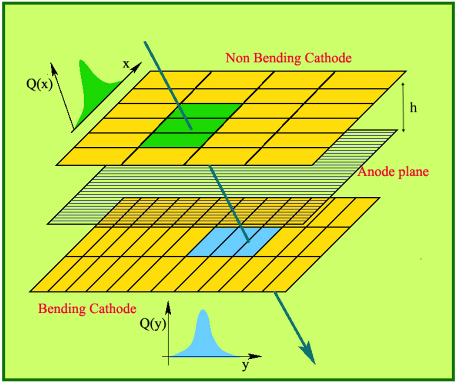

image from Sanjoy Pal

Bending : along with the direction of the magnetic field

- **M**ulti **W**ire **P**roportional **C**hamber (MWPC)
- h : anode-cathode separation distance
- Cathodes planes segmented into pads (Cathode Pad Chamber)
- Bending $\Rightarrow \Delta Y = $ cste
- Non Bending $\Rightarrow \Delta X = $ cste
- Charge deposition on pads $\Rightarrow$ cluster

Context - Charge distribution properties

- Charge distribution in a MWPC has been shown to follow a **Mathieson-Gatti** distribution (normalized and centered at μ):

$$\rho(\lambda = \frac{x}{h}) = 2K_1 \frac{1 - tanh^2(K_2(\lambda - \mu))}{1 + K_3 tanh^2(K_2(\lambda - \mu))}$$

due to symmetry, K_1 and $K_2 = \mathrm{f}(K_3)$.

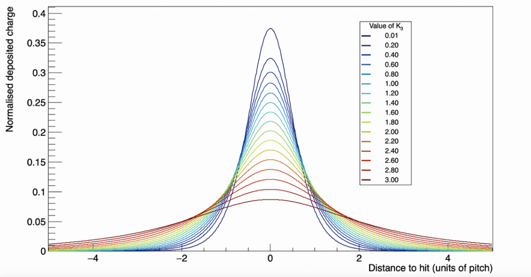

- For a cathode **plane** :

$$\rho(\lambda_X, \lambda_Y) = \rho(\lambda_X)\rho(\lambda_Y) \Rightarrow Cov(X, Y) = 0$$

Context - Clusters & tracks

- Reconstruction of cluster's coordinates by fitting the pad charge distributions with a Mathieson-Gatti function with fixed K_{3X} and K_{3Y}
- Clusters are then combined to reconstruct the muon tracks

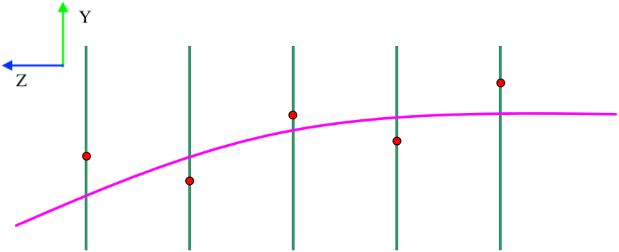

$\rightarrow$ The plane ZY is the most important one

$$p[GeV/c] = 0.3B[T]\rho[m]$$

Context - Goal

- The shape of the Mathieson-Gatti function used in ALICE software is fixed
- BUT these shapes do not reproduce the measured pad charge distributions
- Using better shapes $\rightarrow$ improve clusters $\rightarrow$ improve the invariant mass resolution
- From a selection of data $\rightarrow$ extract K_{3Y} and compare the spacial resolution with the previous one

PROCEDURE

Procedure - Data selection

Selections :

- Run 3 (2022), p-p $\sqrt{s} = 13.6 TeV$
- Track selections :
  $\rightarrow$ $p_{tot} > 10 GeV$
  $\rightarrow$ Tracks within $\eta \in]-4; -2.5[$
  $\rightarrow$ Must match with the **M**uon **Id**entifier
  $\rightarrow$ Reconstructed track close to the primary interaction vertex
- cluster selections :
  $\rightarrow$ Clusters from chamber's parts that don't have a low HV
  $\rightarrow$ **Single** Cluster
  $\rightarrow$ Bending & non-bending planes hit
  $\rightarrow$ A charge asymmetry ($\left|\frac{Q_B - Q_{NB}}{Q_B + Q_{NB}}\right|$) less than 0.5

Procedure - Clusters size

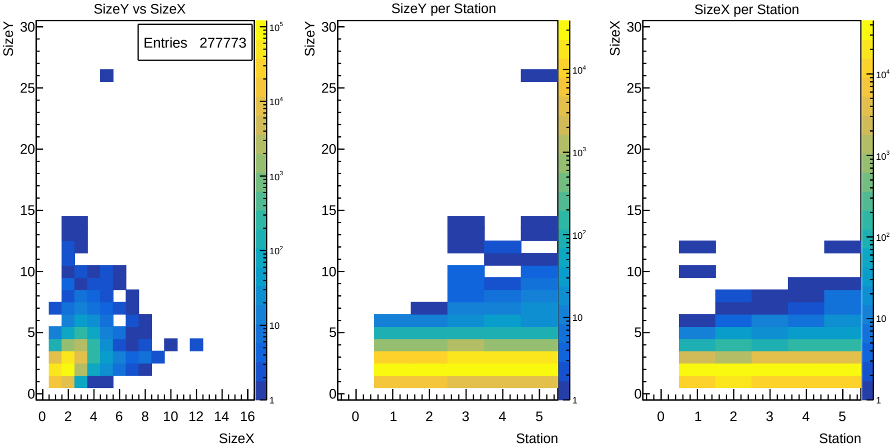

Informations on the selected clusters of the RUN3

→ Most of the selected clusters have a size between 1-3 pads

Procedure - Fitting methods

- Use MLS / LS methods for fitting with *Minuit2/MIGRAD* as a minimizer:

$$\chi^2(\boldsymbol{\theta}) = \sum_{i=1}^{N} \frac{(q_i - f_i(\boldsymbol{\theta}))^2}{\sigma_i^2}$$

$\rightarrow f_i = \mathrm{E}[\mathrm{q}_i]$ *and* $\boldsymbol{\theta} = \{X, Y, K_{3Y}\}$ *estimate parameters*
$\rightarrow$ *MLS* $\equiv \sigma_i = \sqrt{q_i}$ *and LS* $\equiv \sigma_i = \sqrt{f_i}$ (Poisson distribution)

- It is also possible to estimate the number of total charge withing cathode adding a new parameter to $f_i(\boldsymbol{\theta}) \rightarrow f_i(\boldsymbol{\theta}, Q_{tot})$ (denoted as LS+ and MLS+)

Procedure - Fitting methods

- **2D (classical)** : Mix bending and non-bending pads together. Free parameters : $\boldsymbol{\theta} = \{X, Y, K_{3Y}\}$ / $\boldsymbol{\theta} = \{X, Y, K_{3Y}\} \& < Q_{tot} >$

$$f_i(\boldsymbol{\theta}) = < Q_{tot} > \int_{\lambda_{X,i}^{min}}^{\lambda_{X,i}^{max}} \int_{\lambda_{Y,i}^{min}}^{\lambda_{Y,i}^{max}} \rho(\boldsymbol{\lambda}; \boldsymbol{\theta}) d\lambda_X d\lambda_Y$$

(*Implemented in ALICE software with MLS method and* $\boldsymbol{\theta} = \{X, Y\}$)

- **1D** : (Only work on the bending plane) project the charges on the Y axis. Free parameters : $\boldsymbol{\theta} = \{Y, K_{3Y}\}$ / $\boldsymbol{\theta} = \{Y, K_{3Y}\} \& Q_{tot,B}$

$$f_i(\boldsymbol{\theta}) = Q_{tot,B} \int_{-\infty}^{+\infty} \int_{\lambda_{Y,i}^{min}}^{\lambda_{Y,i}^{max}} \rho(\boldsymbol{\lambda}; \boldsymbol{\theta}) d\lambda_X d\lambda_Y$$

Methods	1D	2D mixing
MLS	3_B	$3_B + 2_{NB}$
MLS+	4_B (!)[1]	$3_B + 2_{NB}$
LS+	4_B (!)[1]	$3_B + 2_{NB}$

[1]*: only* 1% *of the selected clusters*

PRELIMINARY RESULTS

Preliminary Results - χ^2/n_d selections (2D MLS)

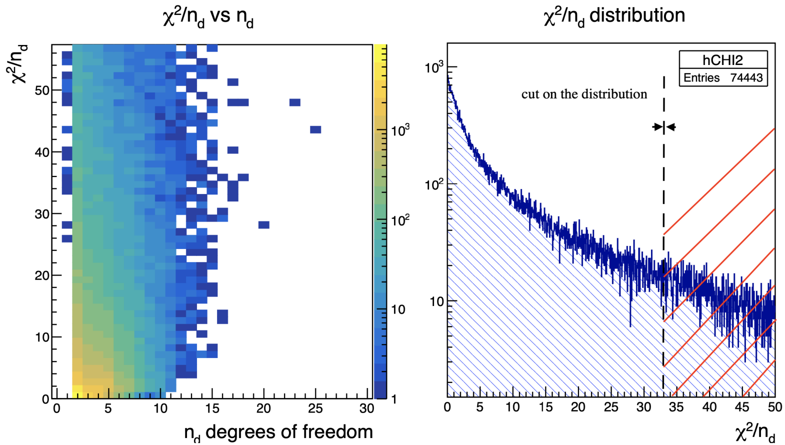

χ^2/n_d results for the 2D MLS method

→ Rejection of "bad" χ^2/n_d set to 7.5% for all methods

Preliminary Results - K_{3Y} distribution for the different methods

→ Pads charge uncertainty

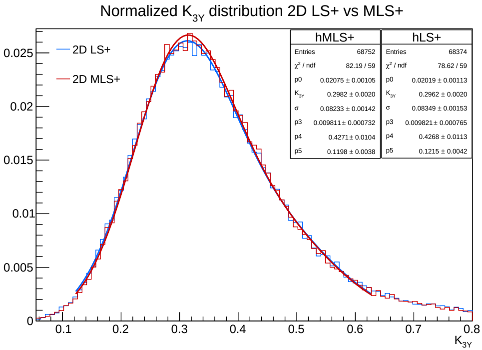

**data fitted with a crystalball function*

Methods	K_{3Y}	$\sigma_{K_{3Y}}$
LS+	0.2962	0.08349
MLS+	0.2982	0.08233

difference between the MLS+ and LS+ method for 2D

Preliminary Results - K_{3Y} distribution for the different methods

$\rightarrow$ Total charge $< Q_{tot} >$ is left free or not

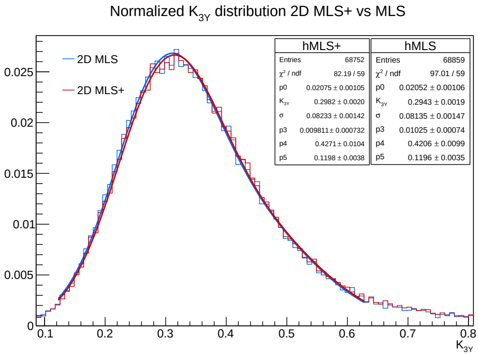

Methods	K_{3Y}	$\sigma_{K_{3Y}}$
MLS	0.2943	0.08135
MLS+	0.2982	0.08233

**data fitted with a crystalball function*

difference between the LS+ and MLS method for 2D

Preliminary Results - K_{3Y} distribution for the different methods

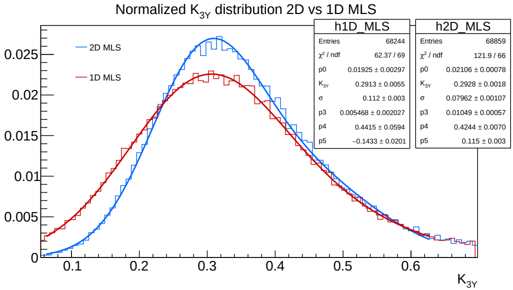

Methods	K_{3Y}	$\sigma_{K_{3Y}}$
2D MLS	0.2928	0.07962
1D MLS	0.2913	0.112

**data fitted with a crystalball function*

difference between the 1D and 2D method for MLS

Preliminary Results - K_{3Y} distribution for the different methods

- Consistency between the methods
- Choice between two methods based on :
  → The lowest standard deviation
  → Keep the one with the least free parameters
-

Methods	K_{3Y}	$\sigma_{K_{3Y}}$
2D MLS	0.2928	0.07962

- **Next step :** influence of others variables on K_{3Y}
  → total charge in bending plane : $Q_{B,tot}$
  → total momentum : p_{tot}
  → fired pads size in bending plane : ΔY
  → angle between the track and the z-axis : φ

Preliminary Results - K_{3Y} vs $Q_{B,tot}$, p_{tot}, ΔY, φ

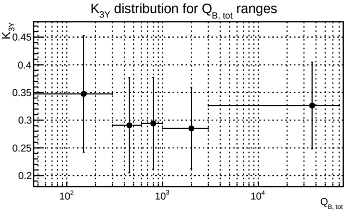

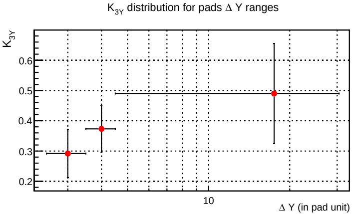

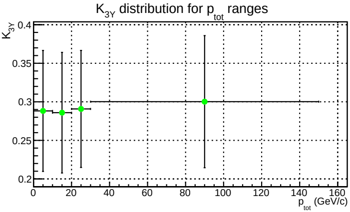

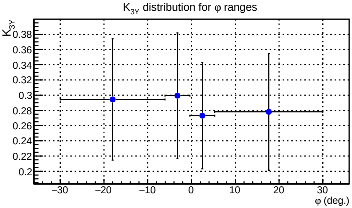

$Q_{B,tot} \rightarrow$ constant

$p_{tot} \rightarrow$ constant

$\Delta Y \rightarrow$ no conclusion (! stats)

$\varphi \rightarrow$ constant

Preliminary Results - K_{3y} distribution per station ($Q_{B,tot} > 300$ ADC & $\Delta Y < 5$)

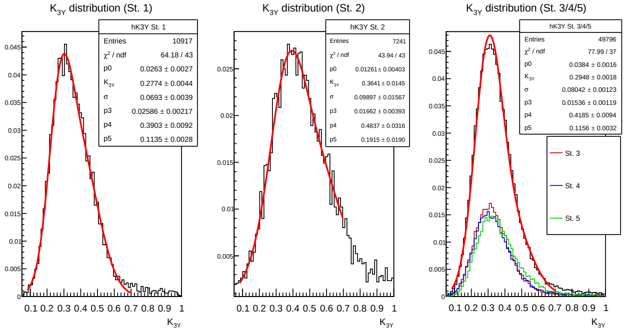

Station	K_{3y}	$\sigma_{K_{3y}}$
St. 1	0.277	0.069
St. 2	0.364	0.099
St. 345	0.295	0.080

Station	old K_{3y}
St. 1	0.570
St. 2	0.584
St. 345	0.584

RESOLUTION

Resolution - Residuals & Resolution

- **Residual :**Δ(track(y)-cluster(y))
- **Spatial Resolution:** σ(Δ(track(y)-cluster(y)))

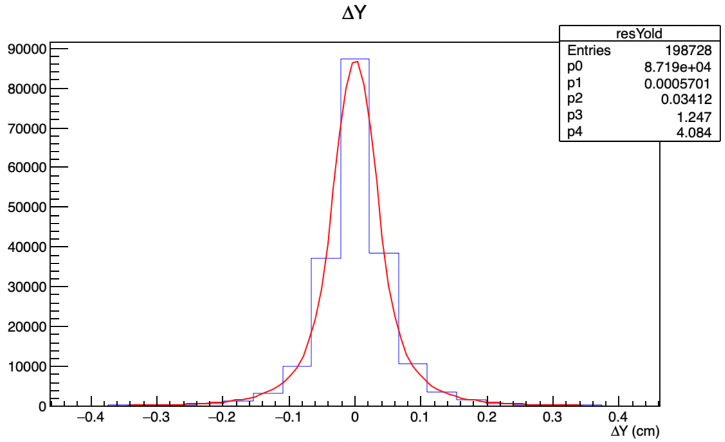

example of the extraction of the spatial resolution from the residuals

- **Blue** points : with the previous values of K_{3Y}.
- **Red** points : with the new ones.

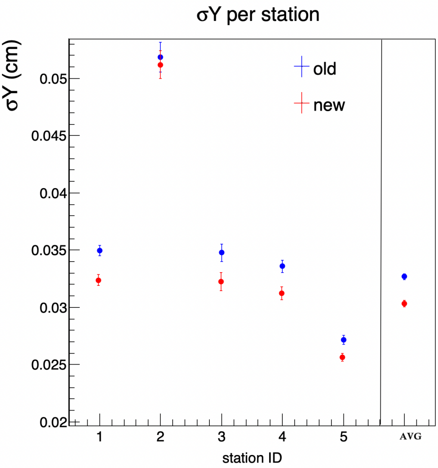

Conclusion & Outlook

- K_{3Y} parameters fitted to the data are smaller than the predicted values
- **Cluster resolution improved** with the new K_{3Y} values :
  $\sigma_{old} = 326.77 \pm 2.72\ \mu m \rightarrow \sigma_{new} = 302.79 \pm 2.64\ \mu m$
  $\Rightarrow$ gain : 7.5%
- Results presented at QGP France and at the next ALICE Muon Week
- The next step is to run the ALICE reconstruction software with the new K_{3Y} parameters and see how much it influences the invariant mass resolution of quarkonia ($\sigma(p) \propto \sigma(Y)p^2$).
- Future studies :
  $\rightarrow$ same procedure for K_{3X}
  $\rightarrow$ charge uncertainty on pads
  $\rightarrow$ review of Mathieson & Gatti function to understand the difference

REFERENCES

References

- Quark-Gluon Plasma : From Big Bang to Little Bang, Yagi et al.,Cambridge University Press ; 2008
- Statistical Data Analysis, Glen Cowan, Owford Science publications, 1998
- E. Gatti *et al.*, Nucl. Instrum. Methods **163** (1979) 83
- E. Mathieson, Nucl. Instrum. Methods **A270** (1988) 602
- ROOT,Minuit 2, https://root.cern.ch/doc/master/Minuit2Page.html
- Addeundum to the ALICE TDR of the dimuon spectrometer, ALICE Collaboration, CERN/LHCC-96-32-LHCC/P3-Addendum 1 1996
- Sébastien Perrin. Study of J/ψ-hadron azimuthal correlations in pp collisions at 13 TeV with ALICE and commissioning of the muon spectrometer. High Energy Physics - Experiment [hep-ex]. Université Paris-Saclay.(2022) tel-03999200
- Rachid Guernane. Optimisation du spectromètre à muons du détecteur ALICE pour l'étude du plasma de quarks et de gluons au LHC. Physique Nucléaire Théorique [nucl-th]. Université Claude Bernard (Lyon, 2001) tel-00001419
- ALICE Collaboration, ALICE upgrades during the LHC Long Shutdown 2, CERN-EP-2023-009 (2023)

BACKUP

Backup

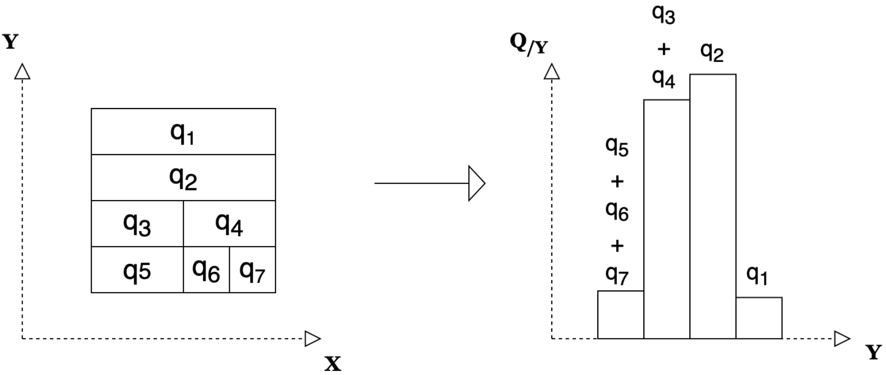

Charge pad projected on the Y-axis

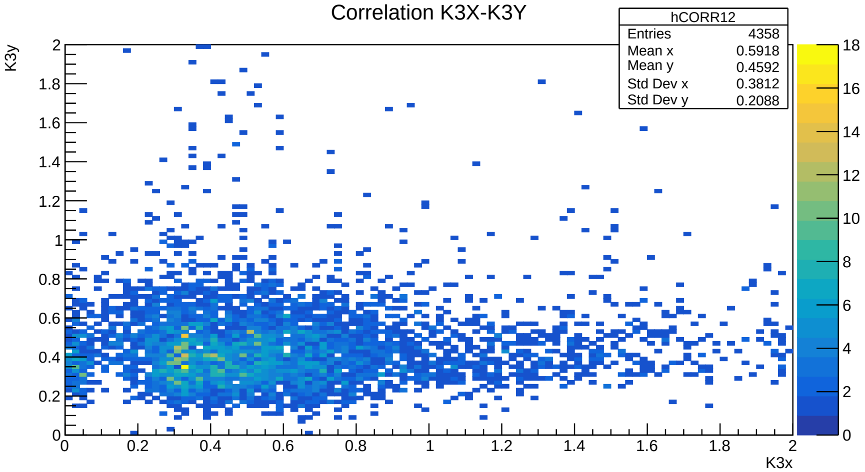

Correlation between K_{3x} & K_{3y}

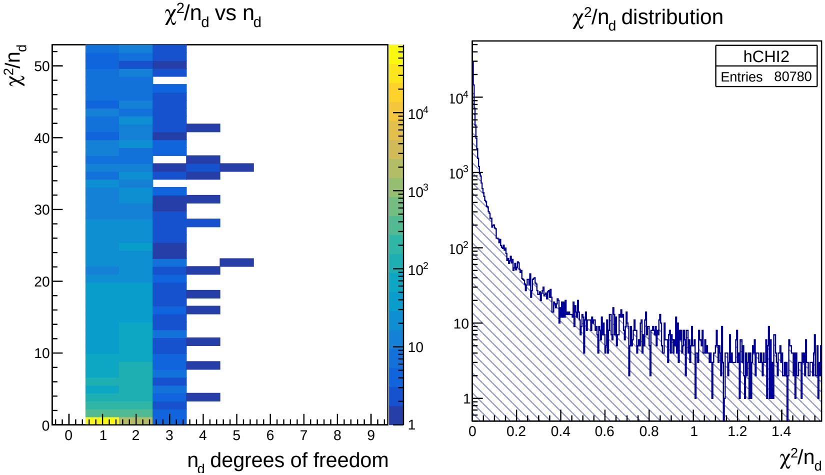

χ^2/n_d results for the 1D MLS method

Backup

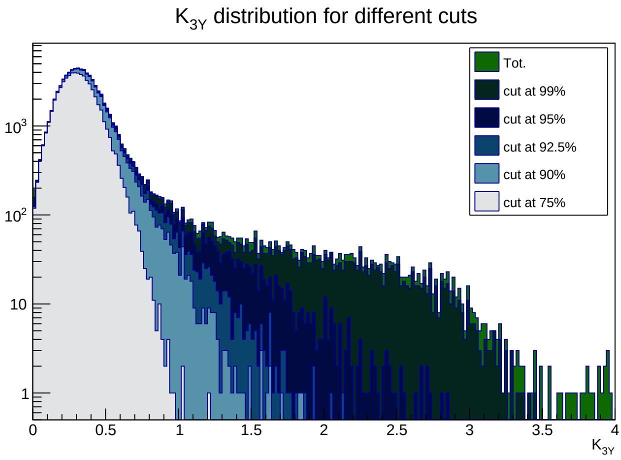

χ^2/n_d results for the 1D MLS method

Backup

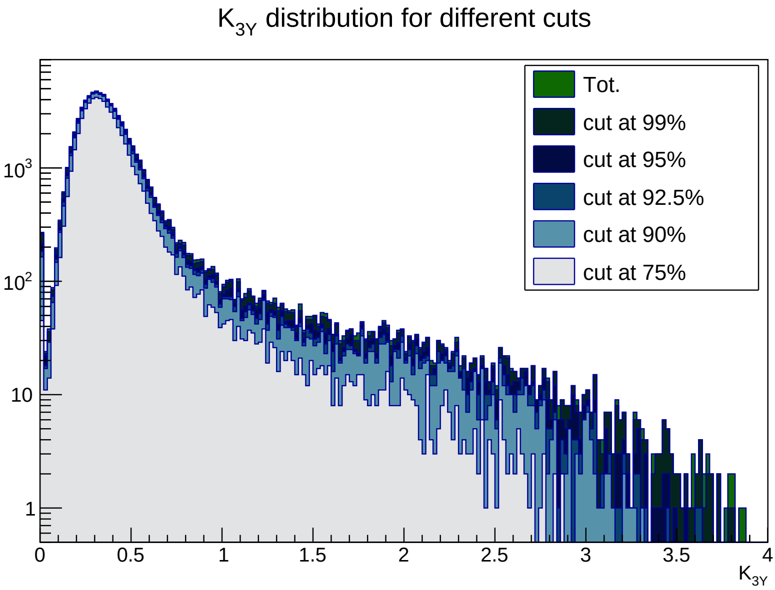

K_{3Y} distribution for different cuts
Tot.
cut at 99%
cut at 95%
cut at 92.5%
cut at 90%
cut at 75%
10^3
10^2
10
1
0
0.5
1
1.5
2
2.5
3
3.5
4
K_{3Y}

Backup

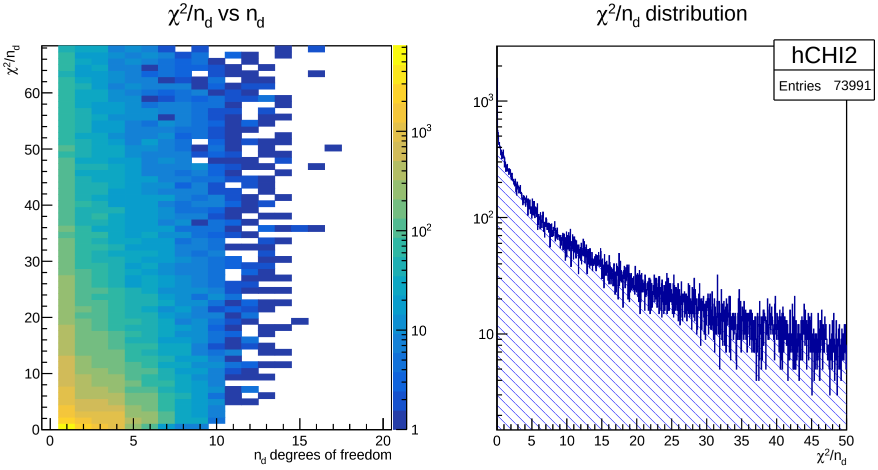

χ^2/n_d results for the 2D LS+ method

Backup

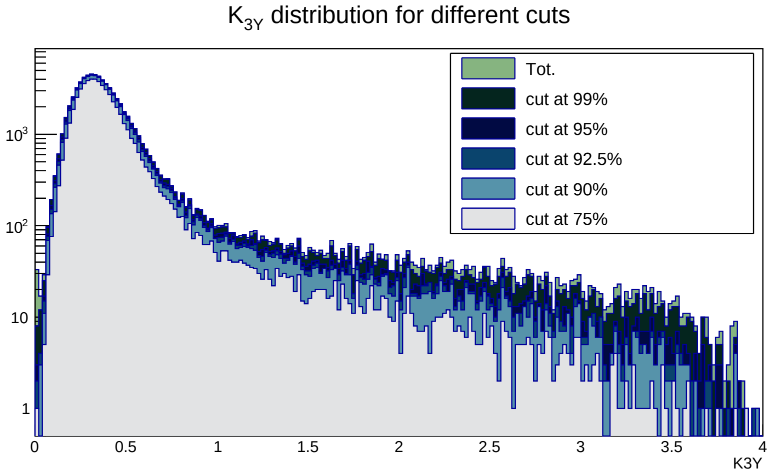

χ^2/n_d cut for the 2D LS+ method

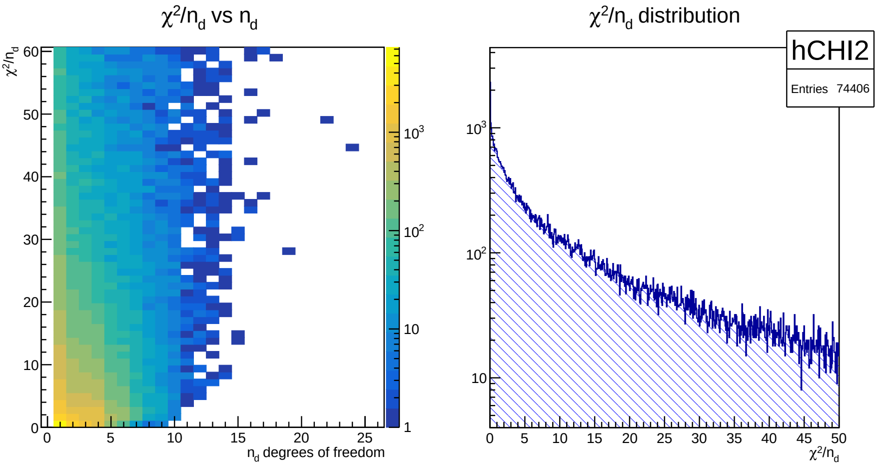

χ^2/n_d results for the 2D MLS+ method

Backup

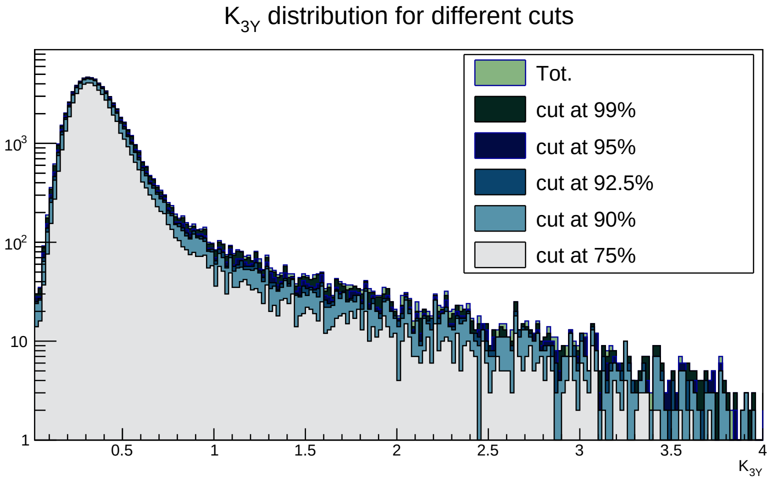

χ^2/n_d cut for the 2D MLS+ method

Backup

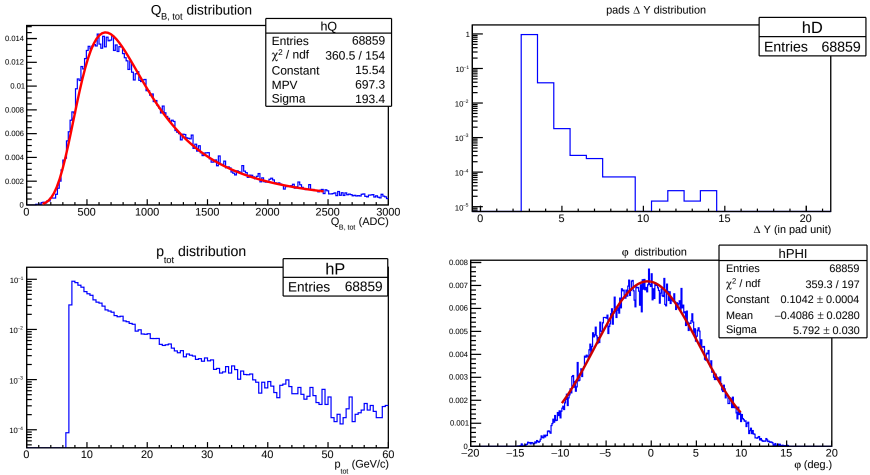

variables distribution

Backup

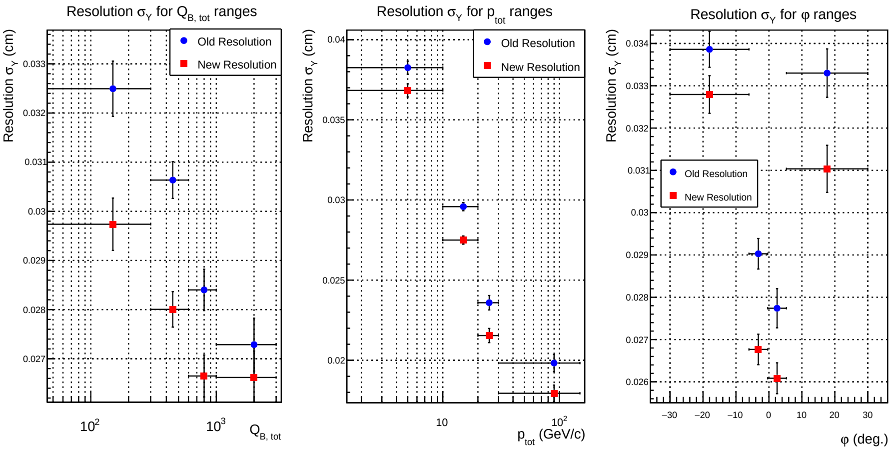

spatial resolution as a function of variable

Backup

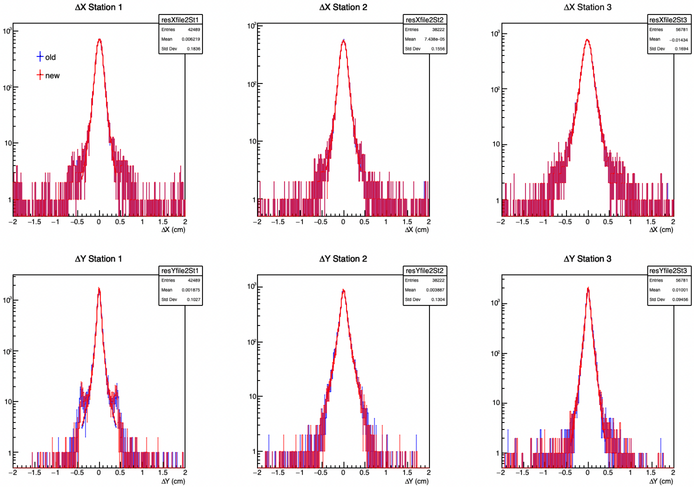

Residuals St. 1/2/3

Backup

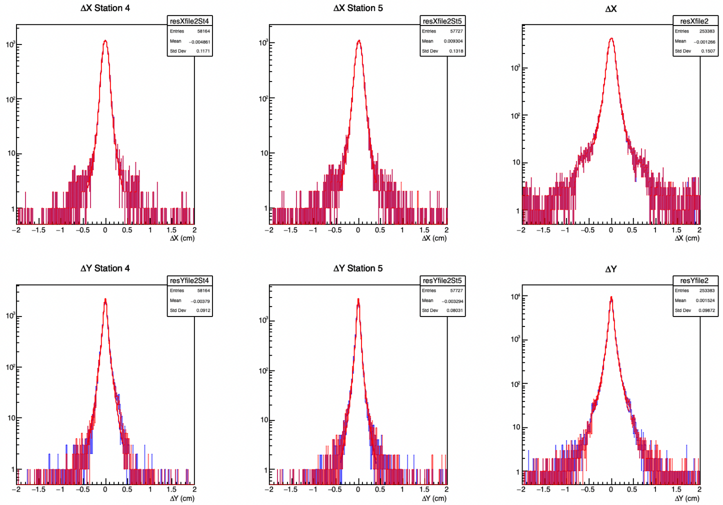

Residuals St.4/5 and tot

Backup

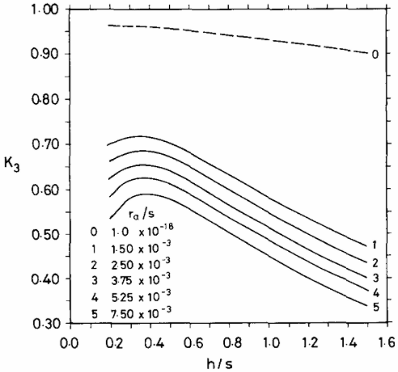

1.00
0.90
0.80
0.70
0.60
0.50
0.40
0.30
K_3
0.0
0.2
0.4
0.6
0.8
1.0
1.2
1.4
1.6
h / s
r_a / s
0 1.0 x 10^{-18}
1 1.50 x 10^{-3}
2 2.50 x 10^{-3}
3 3.75 x 10^{-3}
4 5.25 x 10^{-3}
5 7.50 x 10^{-3}

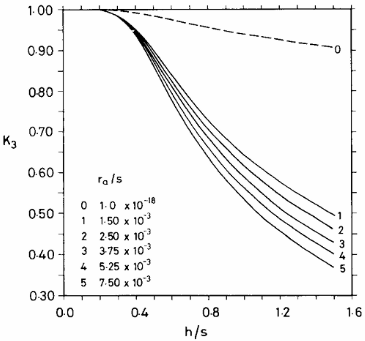

1.00
0.90
0.80
0.70
0.60
0.50
0.40
0.30
K_3
0.0
0.4
0.8
1.2
1.6
h / s
r_a / s
0 1.0 x 10^{-18}
1 1.50 x 10^{-3}
2 2.50 x 10^{-3}
3 3.75 x 10^{-3}
4 5.25 x 10^{-3}
5 7.50 x 10^{-3}

Backup

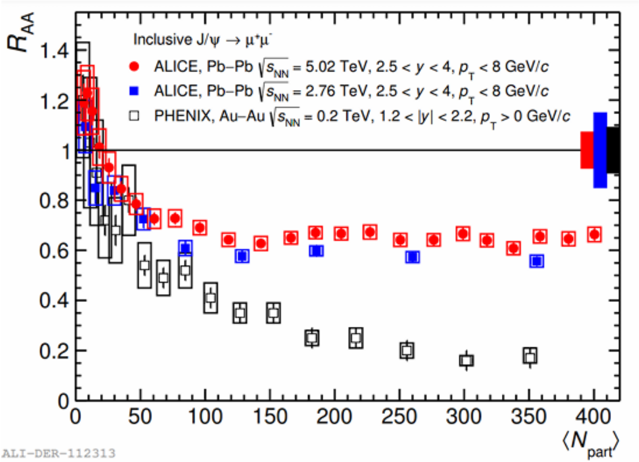

R_{AA}
Inclusive J/ψ → μ⁺μ⁻
ALICE, Pb–Pb $\sqrt{s_{NN}}$ = 5.02 TeV, 2.5 < y < 4, p_T < 8 GeV/c
ALICE, Pb–Pb $\sqrt{s_{NN}}$ = 2.76 TeV, 2.5 < y < 4, p_T < 8 GeV/c
PHENIX, Au–Au $\sqrt{s_{NN}}$ = 0.2 TeV, 1.2 < |y| < 2.2, p_T > 0 GeV/c
0
0.2
0.4
0.6
0.8
1
1.2
1.4
0
50
100
150
200
250
300
350
400
$\langle N_{part} \rangle$
ALI-DER-112313

R_{AA}

Backup

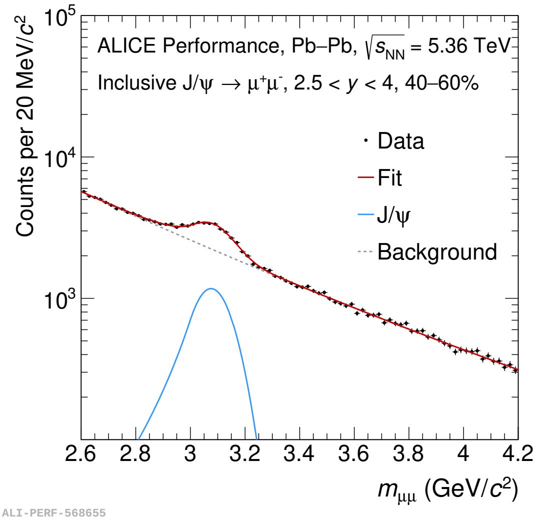

ALICE Performance, Pb–Pb, $\sqrt{s_{NN}}$ = 5.36 TeV
Inclusive J/ψ → μ⁺μ⁻, 2.5 < y < 4, 40–60%
Data
Fit
J/ψ
Background
Counts per 20 MeV/c^2
10^5
10^4
10^3
2.6
2.8
3
3.2
3.4
3.6
3.8
4
4.2
$m_{\mu\mu}$ (GeV/c^2)
ALI-PERF-568655

Backup

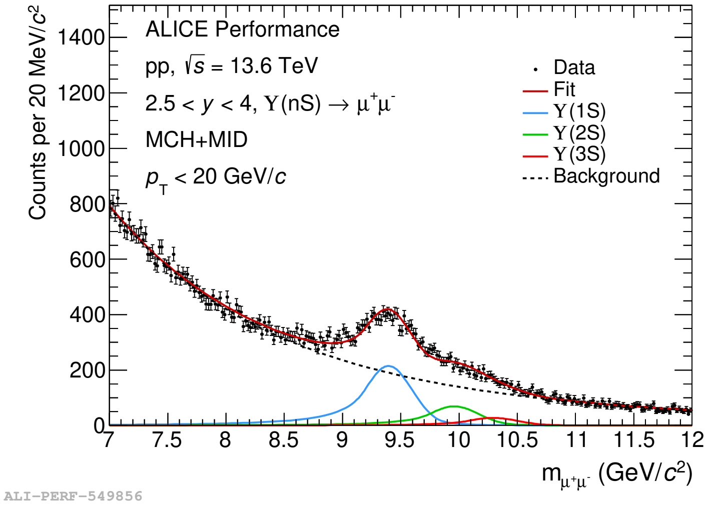

ALICE Performance
pp, √s = 13.6 TeV
2.5 < y < 4, Υ(nS) → μ⁺μ⁻
MCH+MID
p_T < 20 GeV/c
Data
Fit
Υ(1S)
Υ(2S)
Υ(3S)
Background
Counts per 20 MeV/c²
m_μ⁺μ⁻ (GeV/c²)
0
200
400
600
800
1000
1200
1400
7
7.5
8
8.5
9
9.5
10
10.5
11
11.5
12
ALI−PERF−549856